

Optical Detection of the Aharonov-Bohm Effect on a Charged Particle in a Nanoscale Quantum Ring

M. Bayer,^{1,3} M. Korkusinski,² P. Hawrylak,² T. Gutbrod,³ M. Michel,³ and A. Forchel³

¹*Experimentelle Physik II, Universität Dortmund, D-44221 Dortmund, Germany*

²*Institute for Microstructural Sciences, National Research Council, Ottawa, Canada K1A 0R6*

³*Technische Physik, Universität Würzburg, Am Hubland, D-97074 Würzburg, Germany*

(Received 5 November 2002; published 8 May 2003)

We study spectroscopically the current produced by a charged particle moving in a nanosize semiconductor quantum ring subject to a perpendicular magnetic field. Several Aharonov-Bohm oscillations are observed in the emission of a charged exciton confined in a single ring structure. The magnetic field period of the oscillations correlates well with the size of the rings.

DOI: 10.1103/PhysRevLett.90.186801

PACS numbers: 73.21.-b

The phase of a wave function is a fundamental property of quantum systems. One can access and manipulate the phase of a charged object's wave function by placing it in a ring with a magnetic field B perpendicular to it. The vector potential \vec{A} associated with B times the charge Q results in a phase shift that is proportional to the number of flux quanta piercing the ring—the Aharonov-Bohm (AB) effect. It leads to a persistent current of the charge [1] as well as an oscillation of its energy, phenomena which have resulted in considerable theoretical work [2]. Experimental evidence for AB oscillations was available only from transport experiments on metallic/semiconducting rings in the mesoscopic regime, in which the phase coherence might be perturbed by electron-electron, electron-impurity, and electron-phonon scattering [3].

Significant progress has been made by self-assembly of nanosize semiconductor rings. Far-infrared spectroscopy on a macroscopic number of these structures, each of which had been charged with a single electron, was used to measure the transition energy from the ground to the excited electron state as function of the flux quanta number [4]. A change in transition energy with increasing B was reported and attributed to the change of the ground state from a zero angular momentum state to one with angular momentum -1 . In subsequent work [5], interband spectroscopy of a single quantum ring was used to identify neutral and charged exciton complexes, but a true signature of the geometry in the form of AB oscillations has not yet been established.

Here we demonstrate several AB oscillations of a charged particle confined in a quantum ring: In photoluminescence experiments, the emission energy of the charged exciton oscillates with increasing magnetic field. The oscillation whose period correlates well with ring geometry is traced mainly to the final state particle of the optical transition.

Figure 1(a) shows a scanning electron micrograph of a quantum ring with an outer radius of ~ 45 nm and an inner radius of ~ 15 nm, giving an average radius $R_0 \sim$

30 nm. The structure was fabricated by lithographic techniques from a 7 nm wide $\text{In}_{0.10}\text{Ga}_{0.90}\text{As}$ quantum well sandwiched between the GaAs substrate and a 20 nm GaAs cap layer. An advantage of these techniques is the possibility to vary the ring geometry over wide ranges, in contrast to self-assembled nanostructures: Here the width of the rings (difference between outer and inner radii) was kept constant ($W \sim 30$ nm), while the average radius R_0 was varied. On the other hand, the optical quality of lithographic structures is inferior compared to self-organized systems due to the open surfaces.

Despite the good control of the ring shape, questions about localization of carriers in sections along the perimeter arise. A localization site with size comparable to the ring width resembles a quantum dot, which as simply connected geometry does not exhibit AB oscillations. A sensitive criterium in this respect is the exciton diamagnetic shift in a magnetic field normal to the ring. It is determined by the extension of the exciton wave function in the ring plane. Localization leads to a wave function squeezing and thus to a reduction of the shift. The comparison with corresponding quantum dot data [6] shows that the diamagnetic shift in “modulated barrier” ring structures [7] is considerably larger than in ring segments: up to $B = 8$ T it is ~ 2.5 meV in rings with $R_0 \sim 30$ nm as compared to ~ 1 meV shift in dots with 30 nm diameter [8]. This indicates that localization effects are negligible in these systems. On the other hand is the shift smaller than in dots with radii equal to the outer ring radius (~ 4 meV up to 8 T) showing the impact of the removed inner ring section.

Lateral nanostructures of modulated barrier type are obtained by etching the GaAs cap layer only while the quantum well remains unetched [7]. The lateral confinement can be understood by considering the resulting potential profile along the heterostructure. In regions where the cap layer was removed, the profile corresponds to an InGaAs quantum well with asymmetric barriers: GaAs on one side, and vacuum on the other. In unetched regions, the profile corresponds to a symmetric well with

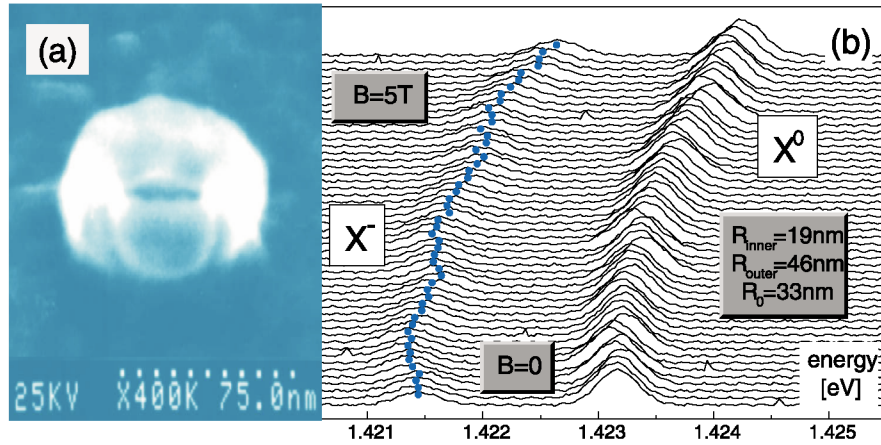


FIG. 1 (color). (a) Electron micrograph of an $\text{In}_{0.10}\text{Ga}_{0.90}\text{As}/\text{GaAs}$ quantum ring. On top, the metallic mask produced by lithography before etching is seen. (b) Circularly polarized photoluminescence spectra of a single ring with an average radius R_0 of 33 nm for different magnetic fields.

GaAs barriers on both sides (disregarding the finite cap width). Because of the larger barrier height, the levels in the asymmetric well region are located at higher energies than those in the symmetric well. This difference in energy creates a lateral confinement with a height of a few tens of meV.

For optical studies, single quantum ring structures were inserted at $T = 2$ K in a split-coil magnetocryostat in the Faraday configuration ($\vec{B} = \vec{B}e_z$). Low power densities were used for optical excitation by an Ar^+ -ion laser, to avoid many-particle effects. The emission was dispersed by a double monochromator ($f = 0.6$ m per stage) providing a spectral resolution of $25 \mu\text{eV}$. Detection was done by a charged coupled devices camera.

Figure 1(b) shows photoluminescence spectra of a single quantum ring with $R_0 \sim 33$ nm for varying magnetic fields. The zero-field spectrum is dominated by two features: a strong emission line and a comparatively weak line shifted by 1.7 meV to lower energies [9]. We attribute the high-energy line X^0 to charge neutral exciton recombination, while we assign the low energy line to emission from charged excitons [10]. The additional carrier in the nominally undoped samples might arise from the non-resonant excitation or from an impurity in the ring environment. From the data, it cannot be clarified whether the exciton complex is negatively or positively charged. For simplicity, we will assign it in the following to X^- .

The evolution of the lines in magnetic field is given by the diamagnetic shift plus the Zeeman spin splitting, which is, however, small for the given nanostructure parameters (< 0.1 meV at 6 T) [11]. For better resolution, the spectra in Fig. 1(b) are represented as a color contour plot in Fig. 2. For the exciton, we observe a smooth shift to higher energies with increasing B as in a simply connected geometry. No indications of AB oscillations are observed within the experimental accuracy. The exciton as a charge neutral particle is not sensitive to magnetic flux. Only higher order quantum effects were predicted [13] to lead to small oscillations of the exciton energy with magnetic field [14]. These fragile oscillations are expected to be extremely small when the finite ring width is regarded [16].

In contrast, the charged exciton has been suggested to undergo AB oscillations [12]: X^- decays into a photon and an electron. The photon energy is equal to the energy difference of the charged exciton and the electron in the initial and final states of the decay: $\hbar\omega = E(X^-) - E(e^-)$. Initial and final state particles are negatively charged, so both their energies should oscillate with magnetic field, but how do these oscillations translate into the photon energy? In experiment, clear signatures of oscillations appear in the field dispersion of the charged exciton emission (the solid dots). Figure 3(a) shows the X^- energy after the B^2 dependence of the diamagnetic shift has been subtracted, from which the oscillatory behavior becomes evident. The oscillations appear to be periodic in magnetic field with a period $\Delta B \sim 1.7$ T. The solid line is the energy calculated for an electron (see below) which is in antiphase with the measured energy.

To attribute the observations uniquely to penetration of magnetic flux $\Phi = \int \vec{B} d\vec{A}$ through the ring, we have tilted the field relative to the ring normal, which reduces the

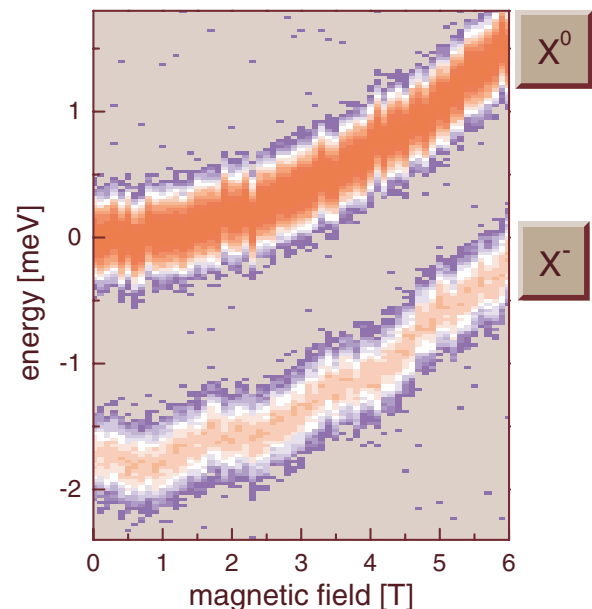


FIG. 2 (color). Contour plot of the spectra shown in Fig. 1.

flux by a factor $\cos\vartheta$, where ϑ is the angle between field and normal. To recover the flux for perpendicular field orientation ($\vartheta = 0$), higher field strengths need to be applied. The period ΔB of the AB oscillations should increase correspondingly. Figure 4(a) shows the related experimental data for ϑ up to 45° . ΔB increases with tilt angle as $1/(\cos\vartheta)$, in agreement with the expectations (the solid line). A flux reduction can also be obtained by a reduction of the ring area, giving a dependence of ΔB on ring radius as $1/R_0^2$, as confirmed in Fig. 4(b) which shows the plot “field period versus ring radius.”

For analyzing these results, we need to understand the role of the initial (X^-) and final (e^-) state particles. In effective mass approximation, the Hamiltonian of X^- is that of two electrons with effective mass m_e , charge $-e$, and coordinates $\vec{r}_{e,i}$ ($i = 1, 2$), and a hole with effective mass m_h , charge $+e$, and coordinate \vec{r}_h :

$$\mathcal{H} = \sum_{i=1}^2 \left[\frac{1}{2m_e} \left(\vec{p}_{e,i} + \frac{e}{c} \vec{A}(\vec{r}_{e,i}) \right)^2 + V_c(\vec{r}_{e,i}) - V_{e-h}(\vec{r}_{e,i} - \vec{r}_h) \right] + \frac{1}{2m_h} \left(p_h - \frac{e}{c} \vec{A}(\vec{r}_h) \right)^2 + V_c(\vec{r}_h) + V_{e-e}(\vec{r}_{e,1} - \vec{r}_{e,2}). \quad (1)$$

The vector potential is given by $\vec{A}(\vec{r}) = \vec{B} \times \vec{r}/2$; $-V_{e-h}(\vec{r}_{e,i} - \vec{r}_h)$ is the attractive electron-hole Coulomb interaction and $+V_{e-e}(\vec{r}_{e,1} - \vec{r}_{e,2})$ is the repulsive electron-electron interaction. The V_c are the geometric ring confinement potentials.

Because of their opposite charges, electrons move in the magnetic field in a direction opposite to the hole but this motion is strongly perturbed by interactions. Since

$$\mathcal{H} = \frac{\sigma}{(1+2\sigma)(1+\sigma)} \left(-i \frac{\partial}{\partial \psi_{c.m.}} + N_\Phi \right)^2 + \sum_{i=1}^2 \left[\left(-i \frac{\partial}{\partial \psi_i} + N_\Phi \right)^2 - \frac{R}{\sqrt{\sin^2(\psi_i/2) + d^2}} \right] + \frac{R}{\sqrt{\sin^2[(\psi_1 - \psi_2)/2] + d^2}} + \frac{\sigma}{(1+\sigma)} \left(-i \frac{\partial}{\partial \psi_1} \right) \left(-i \frac{\partial}{\partial \psi_2} \right) - \frac{2\sigma}{1+2\sigma} N_\Phi^2, \quad (2)$$

with $\sigma = m_e/m_h$. $N_\Phi = \pi R_0^2/(2\pi\ell_c^2)$ is the number of flux quanta through the ring; $\ell_c = (eB/c)^{-1/2}$ is the magnetic length. The transformation separates the correlated motion of the three-particle complex into those of an independent center-of-mass particle and two interacting relative particles with reduced exciton mass μ moving in the attractive potential of a localized point charge. The relative particles interact via Coulomb interactions and via a pairwise, momentum-dependent interaction term. For all of them, the magnetic field enters with the same sign through flux quanta: The c.m. and the relative particles carry the same effective negative charge.

Without interactions, the single particle wave functions are $\chi_m(\psi) = \exp(im\psi)/(2\pi)^{1/2}$, where the integer m gives the angular momentum of the carrier. The only dependence of the wave function on the particle coordi-

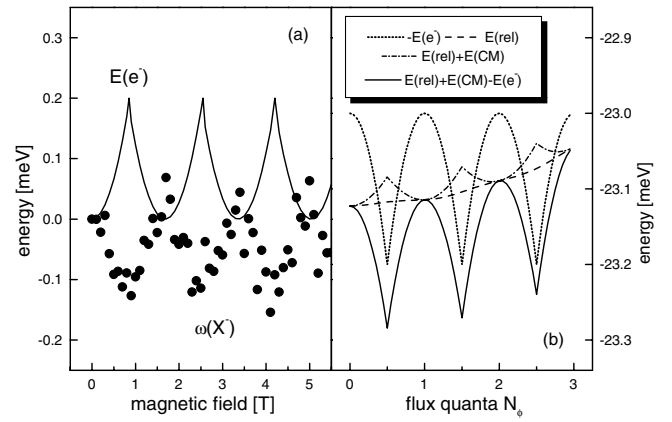


FIG. 3. (a) Measured photon energy from charged exciton recombination (the symbols) plotted against magnetic field after subtracting a fit to the data using a quadratic form. The solid line shows the oscillation of an electron’s energy. (b) Calculated negative electron energy (dotted line), energy of two relative particles (dashed line), total energy of the X^- complex (dash-dotted line), and photon energy (solid line).

the physics addressed here is associated with the motion along the circumference, we study a model ring with infinitesimal width [18]. Thus, the particle positions are restricted to $R_0 \exp(i\varphi)$ with the azimuthal coordinate φ . Further, we adopt for the Coulomb interaction the approximation $V_{e-e}(R, \varphi) = (e^2/2R\epsilon)/[\sin^2(\varphi/2) + d^2]^{1/2}$. Here d prevents the divergence of the Coulomb interaction. Physically it is related to the finite ring width. Transformation to relative coordinates $\psi_i = \varphi_{e,i} - \varphi_h$ and a center-of-mass (c.m.) coordinate $\psi_{c.m.} = m_e(\varphi_{e,1} + \varphi_{e,2})/M + m_h\varphi_h/M$, $M = 2m_e + m_h$, results in [15]

nate is through the phase of the wave function. The single particle eigenenergies are given by $E_m = (m + N_\Phi)^2$. The energy of state m has a minimum for $m = -N_\Phi$. Increasing the number of flux quanta selects states with decreasing angular momenta m as lowest energy level. This is the oscillatory behavior of a charged particle’s energy in a quantum ring subject to a magnetic field.

The X^- wave function is written as product of the c.m. wave function $\Xi_M(\psi_{c.m.}) = \exp(iM\psi_{c.m.})/(2\pi)^{1/2}$ and a superposition of wave functions of the relative particles $\xi^\nu(\psi_1, \psi_2) = \sum_{m_1, m_2} A_{m_1, m_2}^\nu \chi_{m_1}(\psi_1) \chi_{m_2}(\psi_2)$. The eigenstates are obtained by diagonalizing the Hamiltonian matrix [15]. For the ring radius $R_0 = 3$ was chosen corresponding to $R_0 \sim 35$ nm, σ was $1/4$ giving a typical ratio of electron and hole masses.

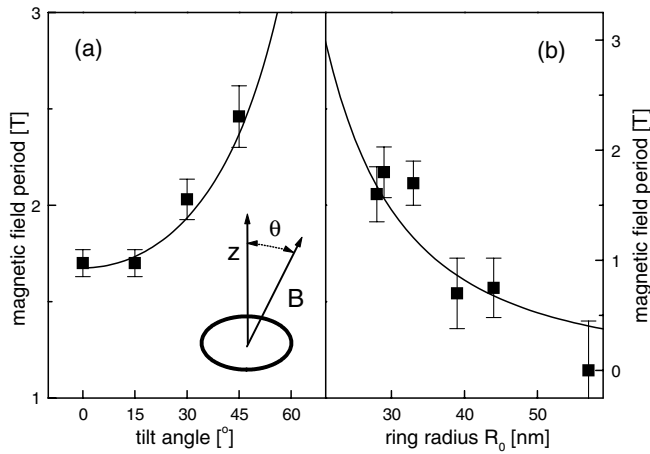


FIG. 4. (a) Magnetic field period of AB oscillations plotted versus tilt angle, as sketched in the inset. (b) Same as (a) but as function of average ring radius. Symbols give experimental data, lines theoretical expectations.

The dependence of the involved energies on the number of flux quanta is shown in Fig. 3(b). The negative energy of an electron $-E(e^-)$ (the dotted line) has smooth maxima at integer flux quanta, and sharp minima at half-integer flux quanta. In contrast, the energy of the relative particle motion (the dashed line) is a smooth function of B , a consequence of the mixing of total angular momenta states by the hole potential. When the energy $E(\text{c.m.})$ of the lowest energy c.m. state is added to that of the X_{rel}^- state, the result shows upward cusps at the maxima of the c.m. energy at exactly half-integer flux quanta (the dash-dotted line). Finally, the photon energy $\hbar\omega = E(X^-) - E(e^-)$ (the solid line) has sharp downward cusps at $N_\Phi = 1/2, 3/2, \dots$ modified by interaction effects. Its behavior is mostly given by the final state electron. The oscillations of X^- lead to a reduction of the oscillation amplitude, for which we find only weak indications in experiment. The period of one flux quantum gives a $\Delta B = 1.7$ T for a ring radius of 28 nm which is within the accuracy in reasonable accord with electron microscopy. Taking the finite ring width into account would lead to mixing not only of azimuthal but also of radial excitations resulting in a further smoothing of the oscillations of the relative particle energies, but this does affect neither period nor phase of the electron oscillations.

This work was supported by the Deutsche Forschungsgemeinschaft, the European Community (IST-FET program CECQDM), and the QuIST program of DARPA.

[1] M. Büttiker, Y. Imry, and R. Landauer, Phys. Lett. **96A**, 365 (1983).

- [2] A. G. Aronov and Yu. V. Sharvin, Rev. Mod. Phys. **59**, 755 (1987); T. Chakraborty and P. Pietiläinen, Phys. Rev. B **50**, 8460 (1994).
- [3] L. P. Lévy *et al.*, Phys. Rev. Lett. **64**, 2074 (1990); V. Chandrasekhar *et al.*, Phys. Rev. Lett. **67**, 3578 (1991); D. Mailly, C. Chapelier, and M. Benoit, Phys. Rev. Lett. **70**, 2020 (1993); A. F. Morpurgo *et al.*, Phys. Rev. Lett. **80**, 1050 (1998); R. Schuster *et al.*, Nature (London) **385**, 417 (1997); A. Fuhrer *et al.*, Nature (London) **413**, 822 (2001); U. F. Keyser *et al.*, cond-mat/0206262.
- [4] A. Lorke *et al.*, Phys. Rev. Lett. **84**, 2223 (2000).
- [5] R. Warburton *et al.*, Nature (London) **405**, 926 (2000).
- [6] M. Bayer *et al.*, Phys. Rev. B **57**, 6584 (1998).
- [7] Ch. Gréus *et al.*, Phys. Rev. B **49**, 5753 (1994).
- [8] Only some modulated barrier rings exhibited diamagnetic shifts, which are large compared to ring segments. For other structures, small shifts were found indicating strong localization, which always is observed in deep-etched [6] rings. Signatures of AB oscillations are found then neither for neutral nor for charged excitons.
- [9] Because of close-by surfaces at which fluctuating charge distributions are created by laser illumination, the spectral lines are quite broad (~ 0.4 meV) compared to self-assembled dots/rings.
- [10] This line cannot be attributed to biexcitonic recombination, as it is observed also at excitation powers at which the average carrier population is clearly below unity.
- [11] The diamagnetic shifts of charged and neutral excitons are comparable. This result is not yet fully understood, since such a behavior would be expected for a strongly confined system with negligible Coulomb correlations only. For systems of rather weak confinement even negative diamagnetic shifts have been predicted [12].
- [12] A. O. Govorov and A. V. Chaplik, JETP Lett. **66**, 454 (1997).
- [13] A. Chaplik, JETP Lett. **62**, 900 (1995); R. A. Römer and M. E. Raikh, Phys. Rev. B **62**, 7045 (2000); J. Song and S. E. Ulloa, Phys. Rev. B **63**, 125302 (2001); H. Hu *et al.*, Phys. Rev. B **63**, 195307 (2001).
- [14] In our model, AB oscillations of the charge neutral exciton with amplitudes much smaller as for the trion occur for weak electron-hole interaction, i.e., strong confinement. These oscillations are quickly smeared out when the interaction cannot be neglected [15].
- [15] M. Korkusinski, P. Hawrylak, and M. Bayer, Phys. Status Solidi B **234**, 271 (2002).
- [16] The exciton does become sensitive to magnetic flux if it has a dipole momentum as for confinement in type-II quantum dots/rings, in which the electron-hole pair is radially polarized. Such structures might be obtained by a proper choice of heterostructure materials or applying an electric field in the radial direction [17].
- [17] A. O. Govorov *et al.*, Phys. Rev. B **66**, 081309 (2002); A. V. Maslov and D. S. Citrin (to be published).
- [18] This assumption is justified by the different energy scales involved in radial and azimuthal quantization, since the ring width is much smaller than its circumference.